Howell et al., http://www.jcb.org/cgi/content/full/jcb.201410095/DC1

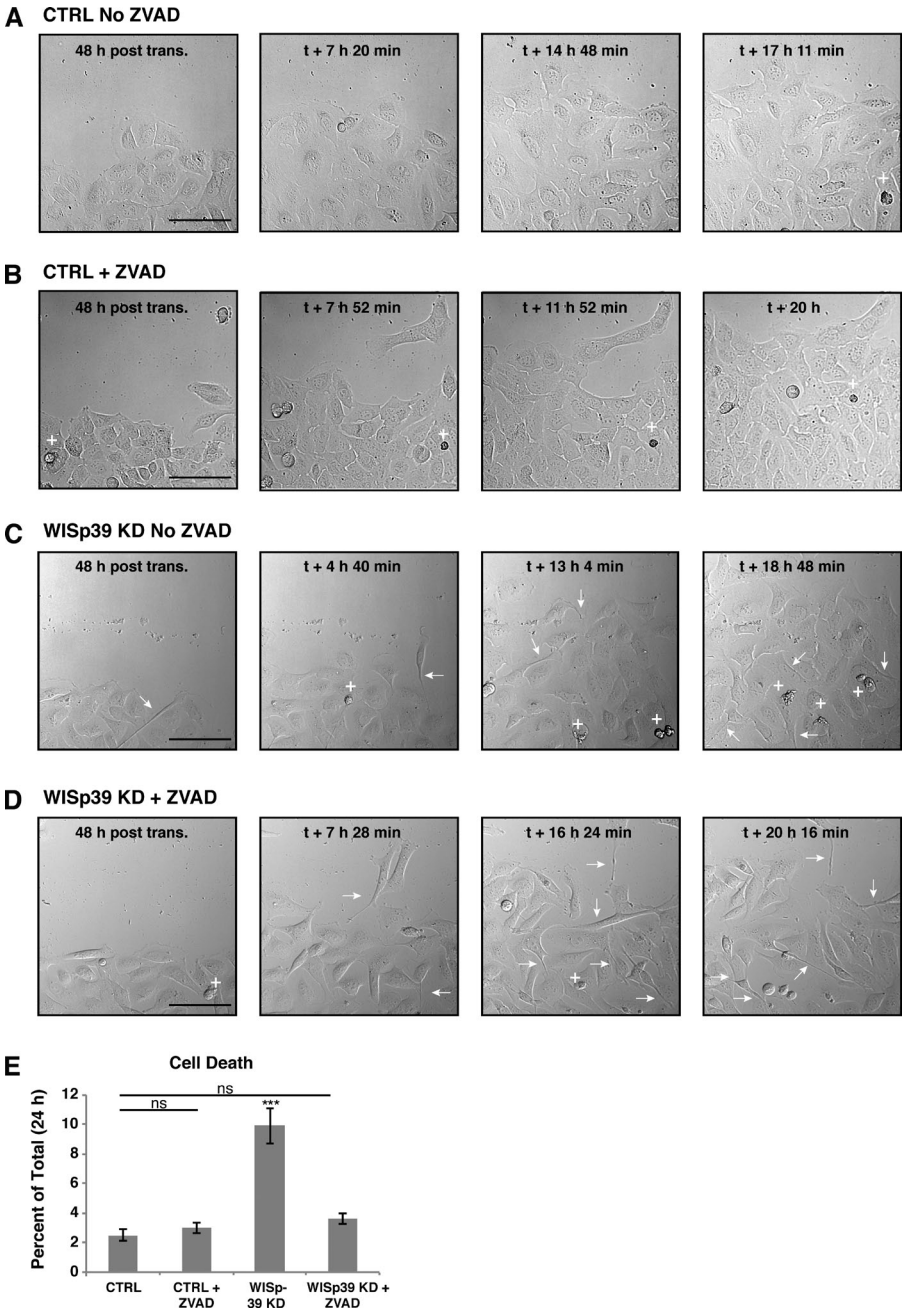

Figure S1. **Abnormal cellular morphology of WISp39 KD is not caused by the stress of undergoing apoptotic cell death.** U2OS cells plated on glass coverslips at confluent density were transfected with either control or WISp39 siRNA for 48 h and then wounded as in Fig. 2. Control or WISp39 KD cells were treated with 100 µM ZVAD to suppress apoptosis, and live-cell migration was imaged starting 48 h posttransfection (post trans.). Crosses, visible dead cell; arrows, visible morphology change caused by WISp39 KD. Bars, 50 µm. (A and B) Control cells showed normal morphology and migration patterns (Videos 3 and 4) with or without ZVAD treatment. (C and D) WISp39 KD cells without ZVAD treatment showed morphological changes and chaotic migration (Video 5) characteristic of these cells and some cell death (C). Treatment with ZVAD suppressed apoptotic cell death in WISp39 KD cells (D) but had no effect on the morphological changes or chaotic migration characteristics (Video 6) in these cells. (E) Quantitation of cell death in WISp39 KD cells. Cell death was assessed by visual assessment of cells, frame by frame, over the 24-h time course of the video. The data shown represent the means ± SD. Student's *t* test; ***, $P \leq 0.001$; ns, not significant. CTRL, control.

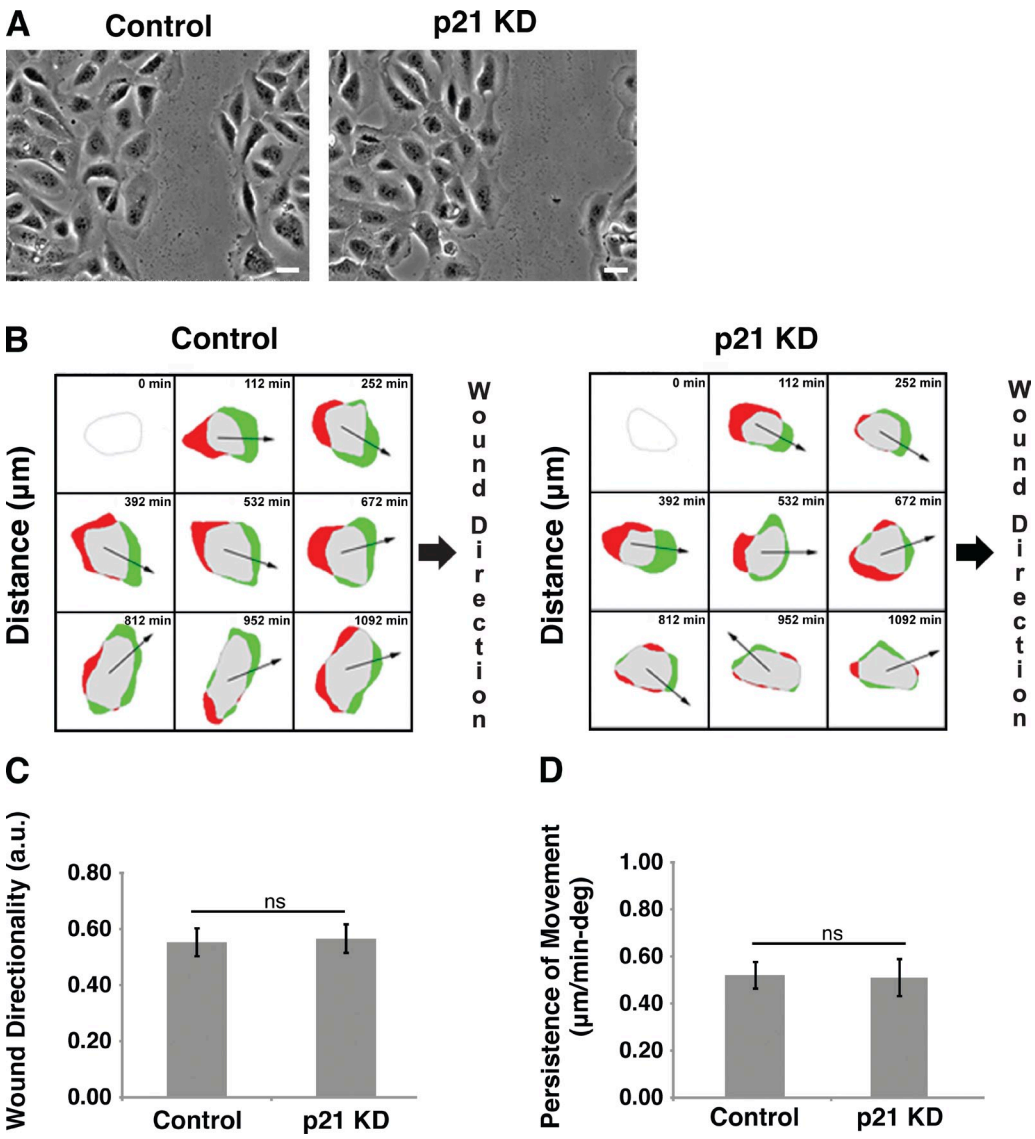

Figure S2. **p21 KD does not promote abnormal cellular morphology or directional migration defects characteristic of WISp39 KD.** (A) U2OS cells plated on glass coverslips at confluent density were transfected with either control or human p21 siRNA (Jascur et al., 2005) for 48 h and then wounded as in Fig. 2. 24 h after wounding, both control cells (left) and p21 KD cells (right) retain cell–cell contact. Bars, 10 µm. (B) Cell protrusion difference diagrams, obtained as in Fig. 2 B, show no change in directionality of individual cells in a wound-healing experiment between control (left) and p21 KD (right). Cells shown are representative examples. (C and D) Quantitation of motility parameters in U2OS cells transfected with control or p21 siRNA. Measurements were performed as described in Fig. 2 and Fig. 3. Number of cells scored from three independent experiments: control (20); p21 KD (20). p21 KD does not lead to any significant change in the parameters. Student's *t* test. a.u., arbitrary unit; deg, degree; ns, not significant.

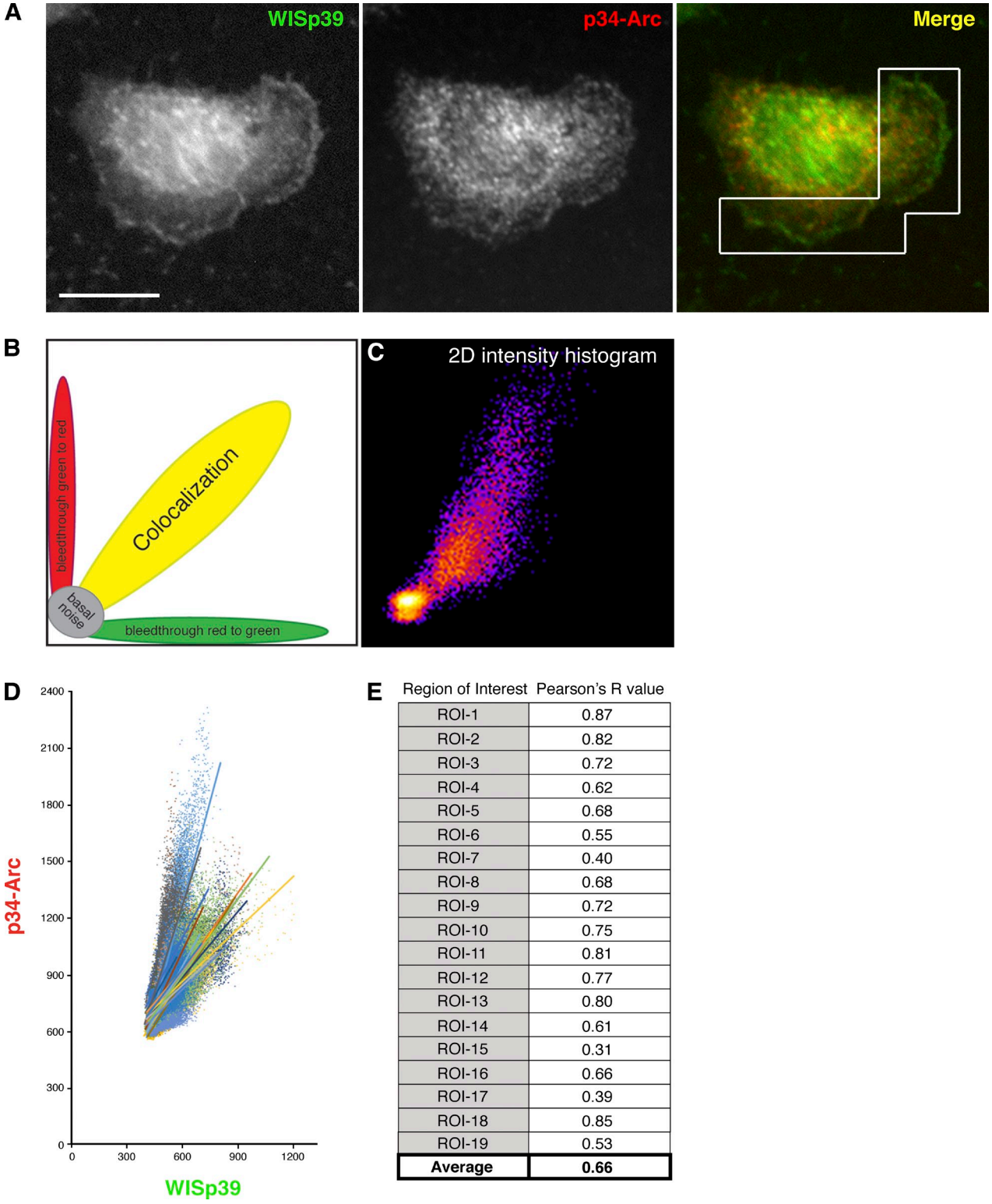

E

Region of Interest	Pearson's R value
ROI-1	0.87
ROI-2	0.82
ROI-3	0.72
ROI-4	0.62
ROI-5	0.68
ROI-6	0.55
ROI-7	0.40
ROI-8	0.68
ROI-9	0.72
ROI-10	0.75
ROI-11	0.81
ROI-12	0.77
ROI-13	0.80
ROI-14	0.61
ROI-15	0.31
ROI-16	0.66
ROI-17	0.39
ROI-18	0.85
ROI-19	0.53
Average	**0.66**

Figure S3. **Colocalization of WISp39 and the Arp2/3 complex at the cell leading edge.** (A) HeLa cells transfected with HA-WISp39 were fixed and stained 30 h later with p34-Arc antibody to detect endogenous p34-Arc and with HA-specific antibodies to detect HA-WISp39. The immunofluorescence images were acquired as described in Materials and methods. The analyzed region of interest is outlined in the merged image. Bar, 10 µm. (B) Schematic representation of colocalization depicted as 2D intensity histogram in C and D (adapted from Bolte and Cordelières, 2006). The intensity of a given pixel in green is plotted along the x coordinate of the scatter plot, and the corresponding intensity of the pixel is plotted in red along the y axis. A tight clustering of pixels around the linear regression line is indicative of a strong correlation between the channels. Its value ranges from 1 to −1, with 1 reflecting complete positive correlation, 0 for no correlation, and −1 for negative correlation. (C) 2D intensity histogram of the region of interest (ROI) defined in A (far right image). (D) 2D intensity histogram of 19 regions of interest analyzed from 17 cells. Pearson's coefficient calculated for the 19 regions of interest analyzed is 0.649 ± 0.17 (SEM), indicative of strong colocalization. The Pearson's coefficient ranges from 1 to −1, with 1 reflecting complete positive correlation, 0 for no correlation, and −1 for negative correlation. (E) Table showing Pearson's coefficient for the 19 regions of interest analyzed.

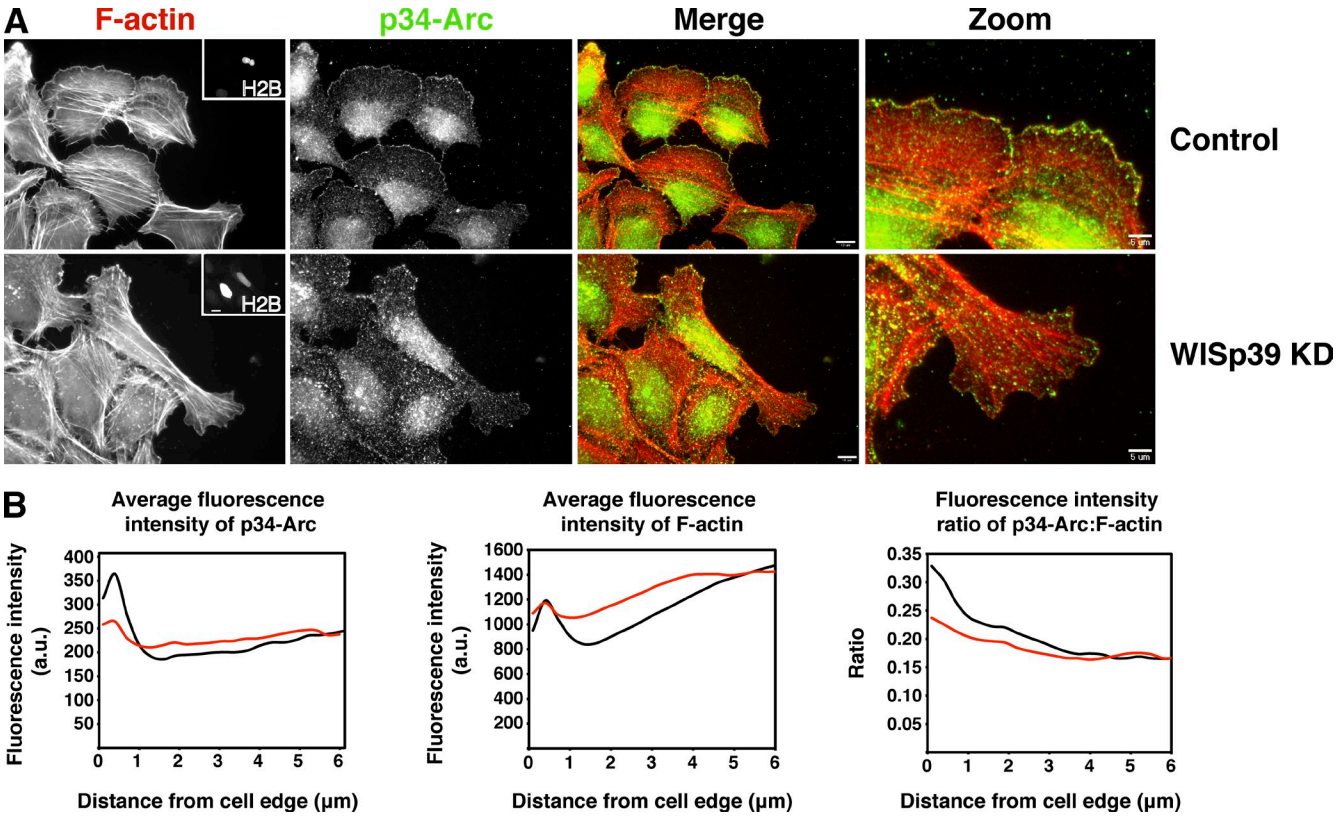

Figure S4. **Additional images and analysis of decreased Arp2/3 complex localization at the cell leading edge in WISp39 KD cells.** (A) WISp39 KD decreases Arp2/3 localization at the cell leading edge. Immunolocalization of Arp2/3 subunit of p34-Arc and F-actin phalloidin staining in cells transfected for 48 h with control or WISp39 siRNA. Cells were also transfected with GFP-H2B. Insets in the first image show the expression of GFP-H2B, cotransfected with the siRNA. Bar, 10 μm. Magnified regions (2×) are shown in the right-most column (Zoom). Bars, 5 μm. (B) Fluorescence intensity of F-actin, Arp2/3 and the ratio of p34-Arc/F-actin in control (black) and WISp39 KD (red) cells, measured from the cell edge (distance = 0) to the cell center (6 μm). For quantification, cells with different lamellipodium sizes were included in the analysis. The data shown represent one experiment and are averaged from $n \geq 18$ cells for each condition. The experiment was repeated three times, with similar results. a.u., arbitrary unit.

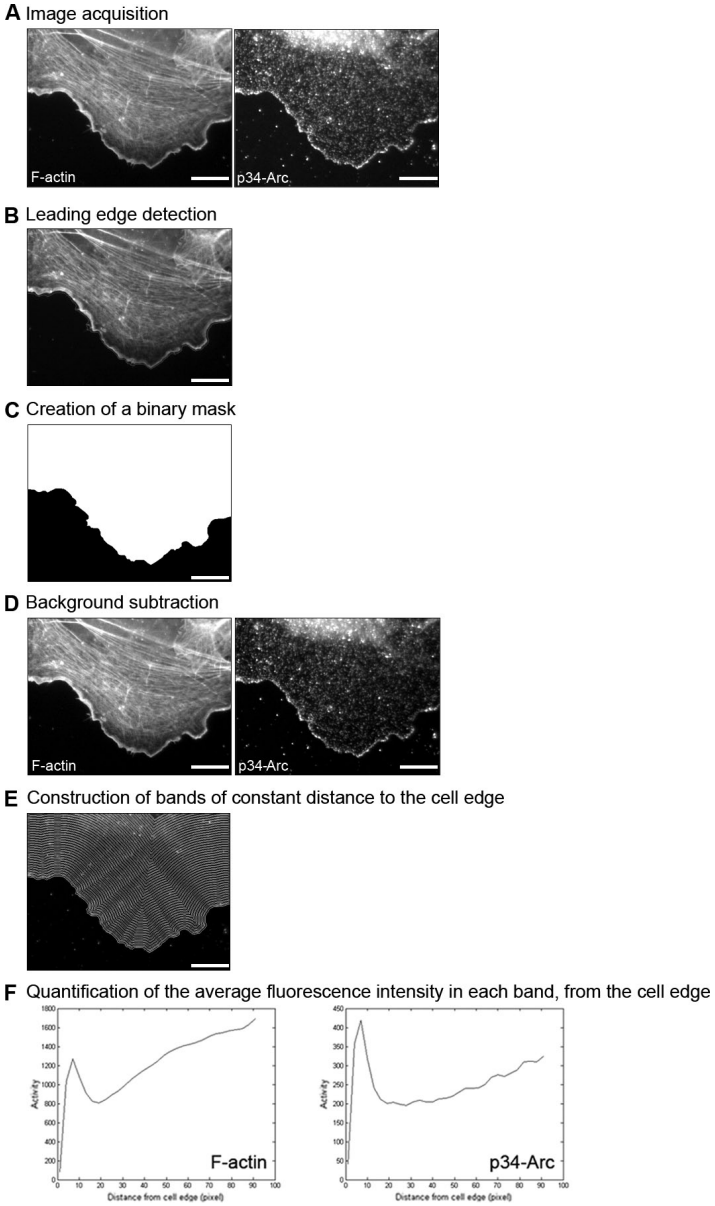

Figure S5. **Quantification of the fluorescence intensity shown in Fig. 6.** Quantification of the fluorescence intensity of F-actin, p34-Arc, and free barbed filament ends as a function of the distance from the cell leading edge was obtained with custom software written in MATLAB (MathWorks). (A) Immunofluorescence images of fixed cells were acquired on an inverted microscope (TE2000-U; Nikon) as described in Materials and methods. Images were cut using MetaMorph software to include only the protrusions. (B and C) Applying the Run Edge Tracker function in fsmCenter in MATLAB, the leading edge of the cell was detected (B), and a corresponding binary mask was created (C). (D) The mask was then used to subtract the background of each set of images, F-actin and p34-Arc, using the Subtract Background function in cytoProbe in MATLAB. (E and F) Bands of constant distance to the cell edge were constructed by running the Activity from Edge function in cytoProbe (E), and individual fluorescence intensities were accumulated and averaged in each band to produce fluorescence intensities versus distance to the cell edge graphs (F). Bars, 10 µm.

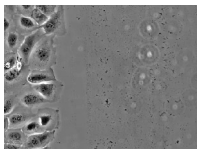

Video 1. **Live-cell imaging of control cells.** U2OS cells were transfected with control siRNA for 48 h and then imaged by time-lapse microscopy using an inverted microscope (TE-200; Nikon). Frames were taken every 7 min for 24 h. Cells show normal apolar morphology and directional migration into the wound.

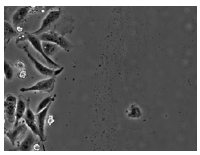

Video 2. **Live-cell imaging of WISp39 KD cells.** U2OS cells were transfected with WISp39 siRNA for 48 h and then imaged by time-lapse microscopy using an inverted microscope (TE-200; Nikon). Frames were taken every 7 min for 24 h. Cells show an increase in bi- and multipolarity with chaotic migration patterns unrelated to wound closure.

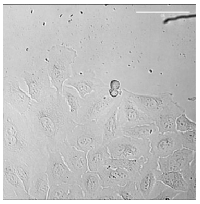

Video 3. **Live-cell imaging of control cells without ZVAD.** U2OS cells were transfected with control siRNA for 48 h then imaged by time-lapse microscopy using an inverted microscope (IX81; Olympus). Frames were taken every 8 min for 24 h. Cells show normal apolar morphology and directional migration similar to Video 1, with few dead cells. Bar, 50 µm.

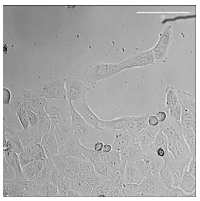

Video 4. **Live-cell imaging of control cells treated with ZVAD.** U2OS cells were transfected with control siRNA for 48 h, treated with 100 µM ZVAD 1 h before imaging, and then imaged by time-lapse microscopy using an inverted microscope (IX81; Olympus). Frames were taken every 8 min for 24 h. Cells showing normal apolar morphology and directional migration similar to Video 3, with few dead cells. Bar, 50 µm.

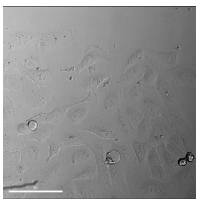

Video 5. **Live-cell imaging of WISp39 KD cells without ZVAD.** U2OS cells were transfected with WISp39 1B siRNA for 48 h and then imaged by time-lapse microscopy using an inverted microscope (IX81; Olympus). Frames were taken every 8 min for 24 h. Cells show an increase in bi- and multipolarity, chaotic migration and increased cell death compared with control cells. Bar, 50 µm.

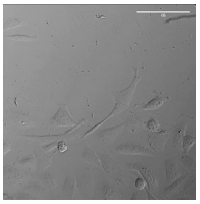

Video 6. **Live-cell imaging of WISp39 KD cells treated with ZVAD.** U2OS cells were transfected with WISp39 1B siRNA for 48 h, treated with 100 µM ZVAD 1 h before imaging, and then imaged by time-lapse microscopy using an inverted microscope (IX81; Olympus). Frames were taken every 8 min for 24 h. Cells continue to show an increase in bi- and multipolarity and chaotic migration, but cell death decreases to control cell levels. Bar, 50 µm.

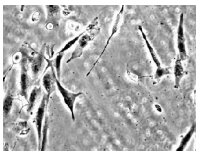

Video 7. **Live-cell imaging of Coronin 1B siRNA-transfected cells.** U2OS cells were transfected with Coronin 1B siRNA for 48 h and then imaged by time-lapse microscopy using an inverted microscope (TE-200; Nikon). Frames were taken every 7 min for 24 h. Cell morphology showing an increase in bi- and multipolarity is similar to WISp39 KD cells.

References

Bolte, S., and F.P. Cordelières. 2006. A guided tour into subcellular colocalization analysis in light microscopy. *J. Microsc.* 224:213–232. http://dx.doi.org/10.1111/j.1365-2818.2006.01706.x

Jascur, T., H. Brickner, I. Salles-Passador, V. Barbier, A. El Khissiin, B. Smith, R. Fotedar, and A. Fotedar. 2005. Regulation of p21(WAF1/CIP1) stability by WISp39, a Hsp90 binding TPR protein. *Mol. Cell*. 17:237–249. http://dx.doi.org/10.1016/j.molcel.2004.11.049